International Journal of Applied Mathematics

Volume 36 No. 4 2023, 537-553

ISSN: 1311-1728 (printed version); ISSN: 1314-8060 (on-line version)

doi: http://dx.doi.org/10.12732/ijam.v36i4.8

ANALYTICAL MODELING ON DISPERSION OF NONCONSERVATIVE POLLUTANT ON A STEP INCREASE IN DEPTH FLOW

Anton Purnama¹§, Easwaran Balakrishnan¹, Khaled S.M. Al-Mashrafi ²

- Department of Mathematics, Sultan Qaboos University Al-Khod PC 123, Muscat, OMAN
- ² Department of Basic Sciences, A'Sharqiyah University PC 400, Ibra, OMAN

Abstract: Coastal wastewater-discharged effluents are likely to consist of pollutants with different dispersion and decay rates that vary with water depth. Mathematical models using a two dimensional advection-diffusion equation with a point source are presented to study the effects of a cross-stream sudden depth change and decay on mixing and dispersing steady discharge of non - conservative effluents. Analytical solutions are illustrated graphically by plotting contours of concentration, showing snapshots of discharged effluent plumes spreading. The shapes of effluent plumes across the cross-stream depth discontinuity line are significantly different, and thus the concentration at the discontinuity line is formulated to measure how much has effluents dispersed into or out of the shallow nearshore region.

AMS Subject Classification: 35Q99, 76R99

Key Words: advection-diffusion equation, flat seabed, far-field model, step seabed, variability of decay

1. Introduction

Steady coastal discharge of wastewater effluents through marine outfall systems into the sea include (treated) municipal wastewaters [1-3], cooling waters [4],

Received: June 1, 2023 © 2023 Academic Publications

and brine effluents [5,6]. Occasionally, due to the desalination plant maintenance, discharged brine effluents may consist of corrosion products, toxic antifoulants and antiscalants [7,8]. These types of nonconservative effluents are subject to (temporal) decay and may contain some unknown (emerging) chemicals, where some of the components are not yet be identified and their toxicity cannot be explained. Decay mechanisms [9,10] include consumption by bacteria or radioactive decay (decay uniform across the flow), heat loss or evaporation through the surface (decay decreasing with depth), and break up or dissolution by turbulence (decay proportional to the flow). For calm sea conditions, the time scales for transverse mixing can be of order a day and thus comparable with the time scales for effluents decay. So, the effect of decay cannot be regarded as a minor perturbation that simply lowers the discharged effluent concentration.

One factor affecting the dilution and spreading of wastewater effluent discharge in coastal waters is the seabed depth profiles [11-15], which are typically ranging between a sloping sandy beach and a mountainous coast with rock sea cliffs, where water depth gets very deep within a short distance from the coast-line. If the discharge of wastewater effluents into the sea cannot be avoided, then it should be done as optimally as possible to ensure that the environmental impact on coastal waters is minimized. Coastal regions and beaches are important for fisheries, local recreation and tourism and for conservation areas.

Modeling studies of the effects of a step increase in depth and decay that decreases or increases with water depth in dispersing steady coastal discharged effluents from a sea outfall in the far-field is investigated analytically using a two-dimensional advection-diffusion equation (see for example [16,17]). The use of model solutions has been a key strategy for the basis of engineering design of marine outfall systems and for assessing the potential impacts. In terms of the practical applicability, it is well recognized that the mathematical model can be applied as benchmark testing to perform preliminary worst-case assessments [16,17,18]. If this easy-to-use assessment indicates no impacts at all, no further action is needed and the use of more sophisticated and time-consuming three-dimensional hydrodynamic and water quality modeling can be avoided.

2. Dispersion of discharged effluents on constant depth flow

Some seabed depth profiles are extremely flat where variations in water depth become insignificant. Therefore, as a reference, we introduce first a highly simplified model of constant depth, and for simplicity, the other complexities,

such as tidal motions, density and temperature, are ignored. The shoreline, which in this case, is a continuation of the rock sea cliffs, is assumed to be straight, and the effluent is discharged at a steady rate Q from a point source at $(x = 0, y = \alpha h_0)$, where $h = h_0$ is an arbitrary reference depth. The (drift) current is assumed to be in the x-direction with speed U_0 at all times. The effluent decay rate is represented by μ_0 , with a typical value up to 0.5 day⁻¹ for decay of faecal in recreational coastal waters [19], decay of dissolved oil (biological consumption of hydrocarbons) [20], and decay of biological oxygen demand [21].

The dispersion processes are represented by the coefficient of dispersivity D_0 , and dispersion in the x-direction is neglected, as the discharged effluent plumes in steady currents become very elongated in the flow direction. The marine outfall systems are commonly installed with multiport diffusers designed to rapidly mix and dilute the discharged effluents with the receiving sea currents, and thus in the far-field modelling, it is also assumed that the effluent concentration is vertically well-mixed over the water depth.

The two-dimensional advection-diffusion equation incorporating a first-order decay for the nonconservative discharged effluent plumes concentration c(x, y) is given by

$$h_0 \mu_0 c + h_0 U_0 \frac{\partial c}{\partial x} - h_0 D_0 \frac{\partial^2 c}{\partial y^2} = Q \delta(x) \delta(y - \alpha h_0), \qquad (1)$$

where the Dirac delta function δ (*) is used to represent the position of a point source at $(x = 0, y = \alpha h_0)$. Note that, the first decay term can be eliminated from Eq. (1) by rewriting $c_* = c \exp(-\mu_0 x/U_0)$. For sufficiently small value of α , to satisfy the no-slip boundary condition at y = 0, an imaginary point source at $(x = 0, y = -\alpha h_0)$ should be added to Eq. (1).

For the graphical representation of solutions, we use dimensionless quantities

$$y = Yh_0$$
, $x = Xh_0$ and $c_*(x, y) = C_*(X, Y) Q/U_0 h_0^2$

and the solution of Eq. (1) for $X \ge 0$ is given by

$$C_* = \sqrt{\frac{\lambda}{4\pi X}} \exp\left\{-\gamma X - \frac{\lambda (Y - \alpha)^2}{4X}\right\},\tag{2}$$

where $\lambda = U_0 h_0/D_0$ represents discharged effluent plumes elongation in the x-direction, and $\gamma = \mu_0 h_0/U_0$ represents the loss rate of discharged effluents. To account for the model application uncertainty and sensitivity due to sea conditions, the values of λ in the range of 0.1-0.3 will be used in the subsequent

plots. Similarly, to reflect the natural small rate of decay μ_0 , the values of γ in the range of 0-0.1 will be used.

The contours of concentration Eq. (2) are plotted in Figure 1 for discharging effluents from a point at $\alpha = 100$, which appear to be almost symmetry about the centerline $(Y = \alpha)$ as if the dispersing plumes do not feel the presence of shoreline. We observe that when $\lambda = 0.3$, the discharged effluent plumes are more elongated. We note also that, due to loss of discharged effluents, contours $(\gamma > 0)$ are significantly smaller than that of conservative effluents with no decay $(\gamma = 0)$. For large effluent decay rates, the remaining portions of the discharged effluent plumes appear not to be advected and dispersed downstream. For smaller values of α , the effect of flow boundary may become significant and the contours slipped towards the shoreline.

The appropriate measure for assessing the environmental impact of discharging effluents into the sea would be the maximum concentration at the shoreline [6,11,13]. A typical standard regulatory criterion would state "does not exceed a certain prescribed safety level of concentration anywhere along the shoreline" to control public health risks in some areas where coastal waters are used for swimming and recreational purposes. After substituting Y=0 in Eq. (2), and by differentiation, it is straightforward to obtain the maximum value of concentration at the shoreline

$$C_{\text{max}} = \sqrt{\frac{\lambda}{4\pi X_{\text{max}}}} \exp\left(-\frac{\sqrt{1+4\lambda\gamma\alpha^2}}{2}\right),$$
 (3)

which occurs at $X_{\text{max}} = \lambda \alpha^2 / \left(1 + \sqrt{1 + 4\lambda \gamma \alpha^2}\right)$. The maximum value is inversely proportional to α , and the result agrees with the standard practice of discharging at a longer offshore distance in order to meet the standard regulatory criterion.

For the case of discharging effluents with no decay ($\gamma = 0$),

$$C_{* \max} = \frac{1}{\sqrt{2\pi e \alpha^2}} \approx \frac{0.242}{\alpha} \text{ and } X_{* \max} = \frac{\lambda \alpha^2}{2}.$$

For example, $C_{*\,\text{max}} < 0.01$ for $\alpha > 25$ and $C_{*\,\text{max}} < 0.001$ for $\alpha > 242$. Thus, by extending a distance $\Delta \alpha$, a relative reduction of the amount $\Delta C_{*\,\text{max}}$ can be formulated as

$$\Delta C_{* \max} = C_{* \max} \left(\frac{\Delta \alpha / \alpha}{1 + \Delta \alpha / \alpha} \right).$$

That is, $C_{*\max}$ is reduced by a third in value when relocating the discharge point to 1.5α , and by a half when extending the discharge point to 2α .

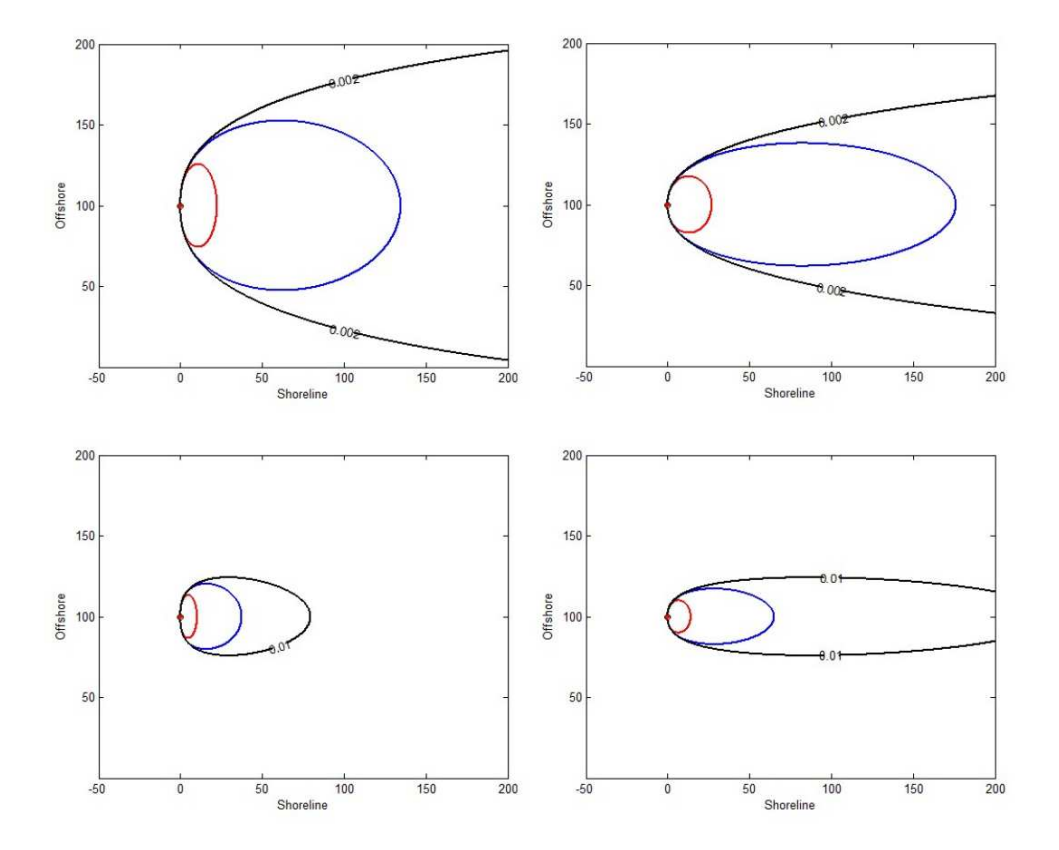


Figure 1: Contours of C=0.002 (top) and C=0.01 (below) for a discharging point source at $\alpha=100$ on constant depth when $\lambda=0.1$ (left column) and $\lambda=0.3$ (right column): no effluent decay $\gamma=0$ (black), $\gamma=0.01$ (blue), and $\gamma=0.1$ (red).

The concentration at the shoreline for discharging effluents from a point source at $\alpha=25$ is shown in Figure 2. Due to loss of discharged effluents, the concentration at the shoreline is significantly reduced as the value γ increases. The position of the maximum concentration is smaller than that of conservative effluents with no decay ($\gamma=0$); and for example, when $\lambda=0.1$, $X_{\rm max}$ decreases from 31.25 for $\gamma=0$ to 10.25 for $\gamma=0.1$. Similarly, when $\lambda=0.3$, the maximum concentration value decreases from 0.01 for no effluent decay ($\gamma=0$) to less than 0.0005 for $\gamma=0.1$.

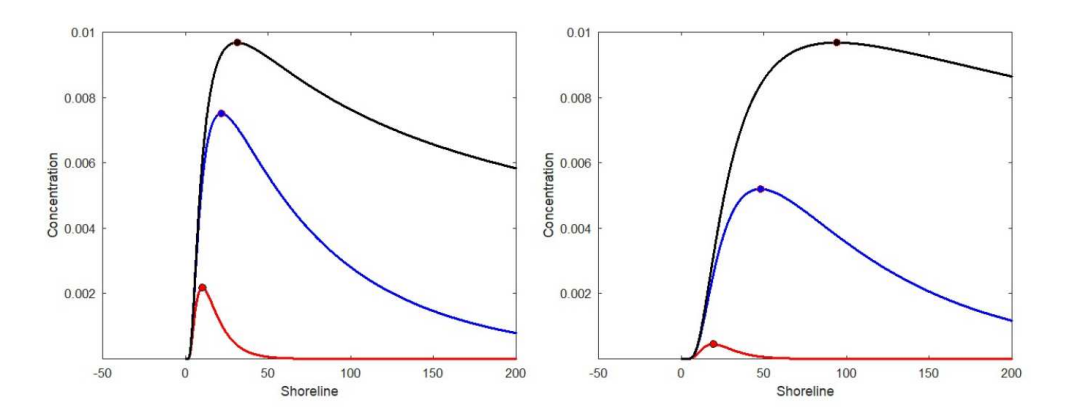


Figure 2: Concentration at the shoreline for discharging effluents from a point source at $\alpha=25$ when $\lambda=0.1$ (left) and $\lambda=0.3$ (right): no effluent decay $\gamma=0$ (black), $\gamma=0.01$ (blue) and $\gamma=0.1$ (red). The maximum value is marked with a dot.

3. Dispersion of discharged effluents on a step increase in depth flow

The sandbags landfill is one of the popular methods to restore and protect the sandy beach erosion from constant wave attack. Due to the pillow shape of sandbags, the beach (face) makeover of piling sandbags creates a profile of steps seabed along the shoreline. In the oceanography textbooks, going further seaward from the shore, the first submerged region is termed continental shelf. The seaward limits of the shelf are determined by the distinct change in depths between the shelf and its adjacent continental slope. Thus, a seabed depth profile is typically depicted as a shallow depth flat seabed coming in contact with a deeper one. As a first attempt to study the effect of variations in water depth, we consider a step increase in depth profile

$$h(y) = \begin{cases} h_0, & 0 \le y < \ell h_0 \\ h_1, & y > \ell h_0 \end{cases},$$

where the sudden cross-stream water depth change occurs at a discontinuity line $y = \ell h_0$ ($\ell > 0$) and $r = h_1/h_0 > 1$ is the ratio of water depths, since $h_1 > h_0$. Note that if r = 1 (and $\ell = 0$), there is no depth change, and it is exactly that of a constant depth $h = h_0$ (and $h = h_1$).

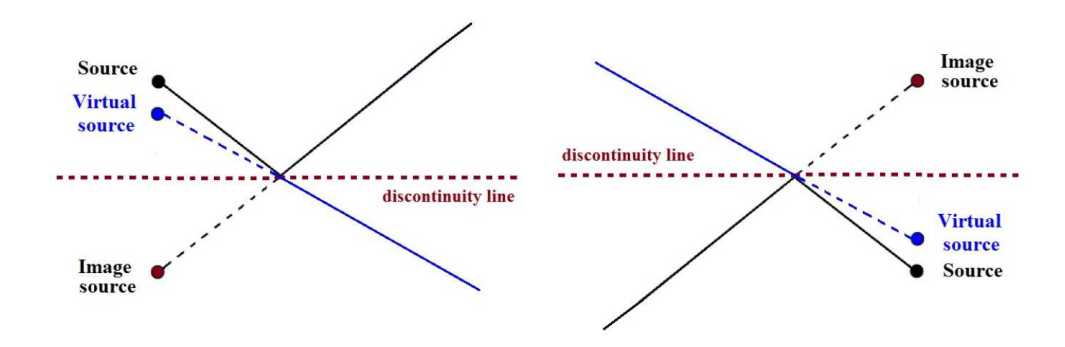


Figure 3: Diagram of the positions of the (actual) point source, image point source, and virtual point source in the method of images, where the discharging point is located in the deeper region (left), and in the shallow region (right).

For a turbulent shallow-water flow over a smooth bed, the variations in the y-direction of current U_1 and dispersivity D_1 are assumed as the power functions only of water depth h [22], and for model application, we take $U_1 = U_0 r^{1/2}$ and $D_1 = D_0 r^{3/2}$ [11,12]. Also, we assume that the discharged nonconservative effluents decay rate μ_1 as a function of water depth in the form $\mu_1 = \mu_0 r^{\sigma+1/2}$ [9,10]. Thus, the effects of loss of discharged effluents that varies with water depth can be illustrated according to the values of σ .

If $\sigma=-1/2$, then $\mu_1=\mu_0$, and the decay rate is independent of water depth. Radioactive decay or consumption by bacteria (at a rate unaffected by sunlight or turbidity) are examples of constant temporal decay. For $\sigma<-1/2$, the decay rate μ_1 decreases with depth. For example, if $\sigma=-1$ then $\mu_1=\mu_0 r^{-1/2}$ represents the decay rate that includes consumption by bacteria which are killed by sunlight at the surface, and air-water exchange (evaporation) at the surface [4,9,10]. For $\sigma>-1/2$, μ_1 increases with depth, and if $\sigma=0$ then $\mu_1=\mu_0 r^{1/2}$ represents the decay rate for the dissolution of oils or break up of clay flocs, which occurs most rapidly in the regions of the flow where the turbulence is energetic. In the subsequent plots, the reference values r=2 and $\sigma=-1/2$ will be used unless stated otherwise.

On writing the discharged effluent plumes concentration, in dimensionless form, as

$$C(X,Y) = \begin{cases} C_0 = C_{0*} \exp\left(-\gamma X\right), & 0 \le Y < \ell \\ C_1 = C_{1*} \exp\left(-\gamma r^{\sigma} X\right), & Y > \ell \end{cases},$$

the solution of a two-dimensional advection-diffusion equation for discharging effluents from a point source at $(X = 0, Y = \alpha)$ can be obtained using the method of image [11,12,14,15]. For example, as illustrated in Figure 3 (right, where the solid lines are considered as rays [12]), if a discharging point source is located in the deeper region, then the equation for $C_1(X,Y)$ is due to the discharging point plus an imaginary point source on the other side of the reflecting line at $Y = \ell$. And the equation for $C_0(X,Y)$ is due to a virtual point source diffusing over the absorbing line at $Y = \ell$.

However, as there can be no discontinuities in either the concentration or its gradient across the line $Y = \ell$, the required additional matching conditions are

$$C_0 = C_1$$
 and $\frac{\partial C_0}{\partial Y} = r^{5/2} \frac{\partial C_1}{\partial Y}$.

The discontinuity line can also be thought of as a "boundary wall" for discharging effluent plumes to cross over and spread into or out of the shallow region. Sea outfalls should be sufficiently long to take the full benefit of stronger current and more depth to dilute discharged effluents. Thus, to study the effect of a sudden depth increase at $Y = \ell$, we consider a large value of ℓ such that the discharged effluent plumes most likely do not feel the presence of shoreline.

3.1. Discharging effluents in the shallow region

We assume for simplicity, a discharging point source at $(X = 0, Y = \alpha)$ where $\alpha < \ell$, which is sufficiently close to the line $Y = \ell$, or else very small parts of the effluent plumes will be able to cross over the discontinuity line.

Using the method of image as illustrated in Figure 3 (left), the advectiondiffusion equation for $C_1(X,Y) = C_{1*} \exp(-\gamma r^{\sigma}X)$ is obtained due to a virtual point source at $(X = 0, Y = \beta_1)$ discharging at a rate b_1 . Thus, in dimensionless form,

$$\frac{\partial C_{1*}}{\partial X} - \frac{r}{\lambda} \frac{\partial^2 C_{1*}}{\partial Y^2} = \frac{b_1}{r^{3/2}} \delta(X) \delta(Y - \beta_1),$$

and the solution for $X \geq 0$ is

$$C_1 = \frac{b_1}{r^2} \sqrt{\frac{\lambda}{4\pi X}} \exp\left\{-\gamma r^{\sigma} X - \frac{\lambda (Y - \beta_1)^2}{4r X}\right\}. \tag{4}$$

The advection-diffusion equation for $C_0(X,Y) = C_{0*} \exp(-\gamma X)$ is obtained by superposition of a point source at $(X = 0, Y = \alpha)$ and an imaginary point

source at $(X = 0, Y = 2\ell - \alpha)$ discharging at a different rate a_1 . So, in dimensionless form, the equation for $C_{0*}(X, Y)$ is given by

$$\frac{\partial C_{0*}}{\partial X} - \frac{1}{\lambda} \frac{\partial^2 C_{0*}}{\partial Y^2} = \delta(X) \left[\delta(Y - \alpha) + a_1 \delta(Y - 2\ell + \alpha) \right],$$

and the solution for X > 0 is

$$C_0 = \sqrt{\frac{\lambda}{4\pi X}} \exp(-\gamma X)$$

$$\times \left[\exp\left\{ -\frac{\lambda (Y - \alpha)^2}{4X} \right\} + a_1 \exp\left\{ -\frac{\lambda (Y - 2\ell + \alpha)^2}{4X} \right\} \right]$$

The matching conditions at $Y = \ell$ are required for calculating a_1 , b_1 and β_1 , and thus, we obtain

$$\beta_1 = \ell - \sqrt{r} (\ell - \alpha), a_1 = \frac{1 - r^2}{1 + r^2}, \frac{b_1}{r^2} \exp(-\gamma r^{\sigma} X) = \frac{2}{1 + r^2} \exp(-\gamma X)$$

and in particular, the concentration in the deeper region Eq. (4) can be rewritten as

$$C_1 = \frac{2}{1+r^2} \sqrt{\frac{\lambda}{4\pi X}} \exp\left\{-\gamma X - \frac{\lambda (Y-\beta_1)^2}{4rX}\right\},\,$$

which is independent of σ , i.e. there are no effects of variability of decay with depth, and it can be interpreted as the portions of discharged effluent plumes that escaping out to the deeper region. Similar to discharging effluents on a constant depth, the effect of loss effluent is represented by decay rate γ . We noted that, for no effluent decay ($\gamma = 0$), then $a_1 + b_1 = 1$; and if there is no depth change r = 1 (and $\ell = 0$), then $\beta_1 = \alpha$, $a_1 = 0$ and $b_1 = 1$. Also for r > 1, $a_1 < 0$, $b_1 < 1$ and $\alpha < \beta_1 < \ell$.

To investigate the effect of a step increase in water depth at $\ell=110$, contours of concentration for discharging effluents from a point source at $\alpha=100$ are plotted in Figure 4. The symmetry about the centerline (see Figure 1) for discharging effluents on a constant depth (r=1) is broken due to the presence of a sudden depth change as some portions of the discharged effluent plumes are escaping into and spreading in the deeper region. The features are more significant due to loss of discharged effluents and a bigger increase in depth, where most of the remaining discharged plumes are dispersing in the shallow region.

Using the contours value of C=0.002, the effects of a step increase in depth are shown on the left column of Figure 4. If the deeper water is three

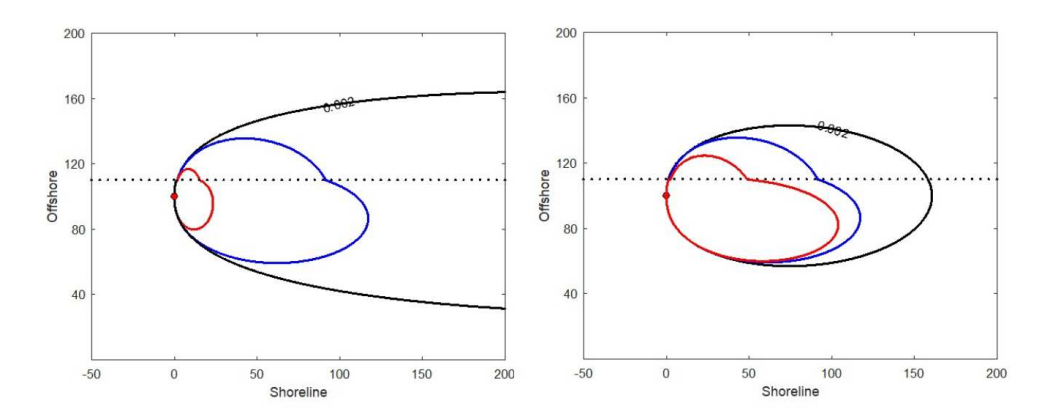


Figure 4: Contours of C=0.002 for a discharging point source at $\alpha=100$ on a step increase at $\ell=110$ when $\lambda=0.2$. (left column) The variation of decay rate when r=3 (top) and r=5 (bottom): no effluent decay $\gamma=0$ (black), $\gamma=0.01$ (blue) and $\gamma=0.1$ (red). (right column) The variation of water depth when $\gamma=0.01$: r=1 (black), r=2 (blue) and r=3 (red).

times longer than that of the shallow (r > 3), the mixing is enhanced and no discharged effluent plumes escaping into the deeper region. The entire plumes are dispersed in the shallow region. The additional effect of discharged effluents decay are illustrated on the right column of Figure 4.

The concentration levels at the discontinuity line $Y = \ell$ play an important role in determining the portions of discharged effluent plumes that crossing over and dispersing into the deeper region. Next, by putting $Y = \ell$, we obtain the concentration at the discontinuity line

$$C_0\left(X,\ell\right) = C_1\left(X,\ell\right) = \frac{2}{r^2 + 1} \sqrt{\frac{\lambda}{4\pi X}} \left[\exp\left\{-\gamma X - \frac{\lambda \left(\ell - \alpha\right)^2}{4X}\right\} \right],$$

which has a maximum value

$$C_{1 \max} = \frac{2}{r^2 + 1} \sqrt{\frac{\lambda}{4\pi X_{1 \max}}} \exp\left(-\frac{\sqrt{1 + 4\lambda \gamma (\ell - \alpha)^2}}{2}\right),$$

at
$$X_{1 \max} = \lambda (\ell - \alpha)^2 / \left[1 + \sqrt{1 + 4\lambda \gamma (\ell - \alpha)^2} \right].$$

In the limit as $\ell \to 0$, we obtain the concentration at the shoreline

$$C_0\left(X,0\right) \approx \frac{2}{1+r^2} \sqrt{\frac{\lambda}{4\pi X}} \exp\left(-\gamma X - \frac{\lambda \alpha^2}{4X}\right),$$

which for r > 1, is $2/(1+r^2)$ smaller than that of constant depth (on substituting Y = 0 in Eq. 2).

For the case of no effluent decay ($\gamma = 0$), the maximum value

$$C_{1 \max} \approx \frac{2}{r^2 + 1} \left(\frac{\alpha}{\ell - \alpha} \right) C_{*max} \text{ and } X_{1 \max} \approx \frac{\lambda (\ell - \alpha)^2}{2}.$$

Note that, if there is no depth change r=1 (and $\ell=0$), then $C_{1\max} \approx C_{*\max}$ and $X_{1\max} \approx X_{*\max}$.

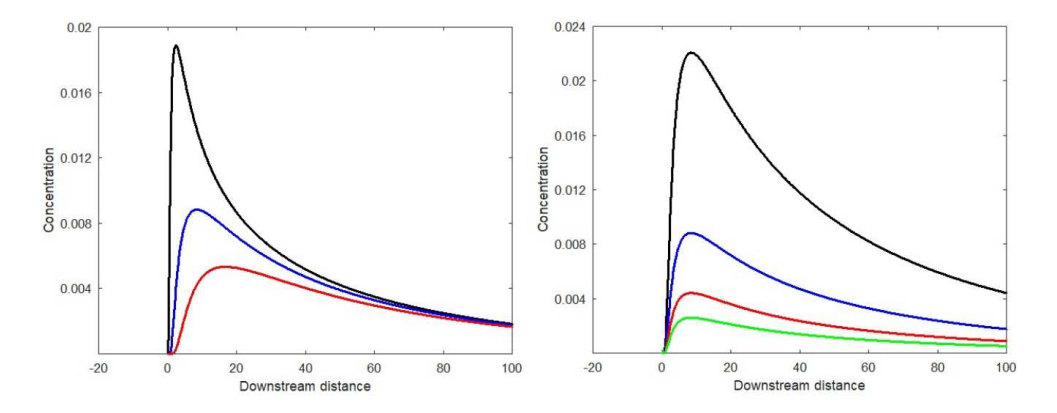


Figure 5: Concentration at the discontinuity line for discharging effluents with $\gamma=0.01$ on a step increase at $\ell=110$ when $\lambda=0.2$: (left) The location of a point source when r=2: $\alpha=95$ (red), $\alpha=100$ (blue) and $\alpha=105$ (black); and (right) The variation of water depth when $\alpha=100$: r=1 (black), r=2 (blue), r=3 (red) and r=4 (green).

The concentration at the discontinuity line for discharging effluents from a point source at $\alpha=100$ with $\ell=110$ and r=2 is shown in Figure 5 (left). The long tail of the graph is the result of the effluent plumes elongation in the downstream direction. The effect of increasing r is shown in Figure 5 (right). Due to small portions of the discharged effluent plumes escaping to the deeper region, the maximum concentration that passes through the discontinuity line decreases from 0.0149 for r=1.5 to 0.0048 for r=3, a decrease of about 68%.

We conclude that, in comparison to discharging effluents from a point source at $\alpha = 100$ on constant depth, the maximum concentration at the shoreline is reduced as a result of a step increase in depth at $\ell = 110$.

3.2. Discharging effluents in the deeper region

For discharging effluents from a point source at $(X = 0, Y = \alpha)$ where $\alpha > \ell$, and using the method of image as illustrated in Figure 3 (right), the advection-diffusion equation for $C_0(X,Y) = C_{0*} \exp(-\gamma X)$ is obtained due to a virtual point source at $(X = 0, Y = \beta_2)$ discharging at a rate b_2 . Thus, in dimensionless form, the equation for $C_{0*}(X,Y)$ is given by

$$\frac{\partial C_{0*}}{\partial X} - \frac{1}{\lambda} \frac{\partial^2 C_{0*}}{\partial Y^2} = b_2 \delta\left(X\right) \delta\left(Y - \beta_2\right),\,$$

and the solution for $X \geq 0$ is

$$C_0 = b_2 \sqrt{\frac{\lambda}{4\pi X}} \exp\left\{-\gamma X - \frac{\lambda (Y - \beta_2)^2}{4X}\right\}.$$
 (5)

The advection-diffusion equation for $C_1(X,Y) = C_{1*} \exp(-\gamma r^{\sigma}X)$ is obtained by superposition of a point source at $(X = 0, Y = \alpha)$ and an imaginary point source at $(X = 0, Y = 2\ell - \alpha)$ discharging at a different rate a_2 ; and thus, in dimensionless form,

$$\frac{\partial C_{1*}}{\partial X} - \frac{r}{\lambda} \frac{\partial^2 C_{1*}}{\partial Y^2} = \frac{1}{r^{3/2}} \delta(Y) \left[\delta(Y - \alpha) + a_2 \delta(Y - 2\ell + \alpha) \right],$$

and the solution for X > 0 is

$$C_{1} = \frac{1}{r^{2}} \sqrt{\frac{\lambda}{4\pi X}} \exp(-\gamma r^{\sigma} X)$$

$$\times \left[\exp\left\{-\frac{\lambda (Y - \alpha)^{2}}{4rX}\right\} + a_{2} \exp\left\{-\frac{\lambda (Y - 2\ell + \alpha)^{2}}{4rX}\right\} \right]$$

From the required matching conditions at $Y = \ell$, we obtain

$$\beta_2 = \ell + \frac{\alpha - \ell}{\sqrt{r}}, a_2 = \frac{r^2 - 1}{r^2 + 1}, b_2 \exp(-\gamma X) = \frac{2}{r^2 + 1} \exp(-\gamma r^{\sigma} X)$$

and thus, in particular, the concentration in the shallow region Eq. (5) can be rewritten as

$$C_0 = \frac{2}{r^2 + 1} \sqrt{\frac{\lambda}{4\pi X}} \exp\left\{-\gamma r^{\sigma} X - \frac{\lambda (Y - \beta_2)^2}{4X}\right\},\,$$

which can be interpreted as the portions of discharged effluent plumes that crossing over the discontinuity line $Y = \ell$ and dispersing within the shallow region. We note that for r > 1, $a_2 < 1$, $b_2 > 0$ and $\ell < \beta_2 < \alpha$. It is also easy to verify that, for no effluent decay ($\gamma = 0$ and $\sigma = 0$), then $a_2 + b_2 = 1$; and if there is no depth change r = 1 (and $\ell = 0$), then $\beta_2 = \alpha$, $\alpha_2 = 0$ and $\alpha_2 = 0$.

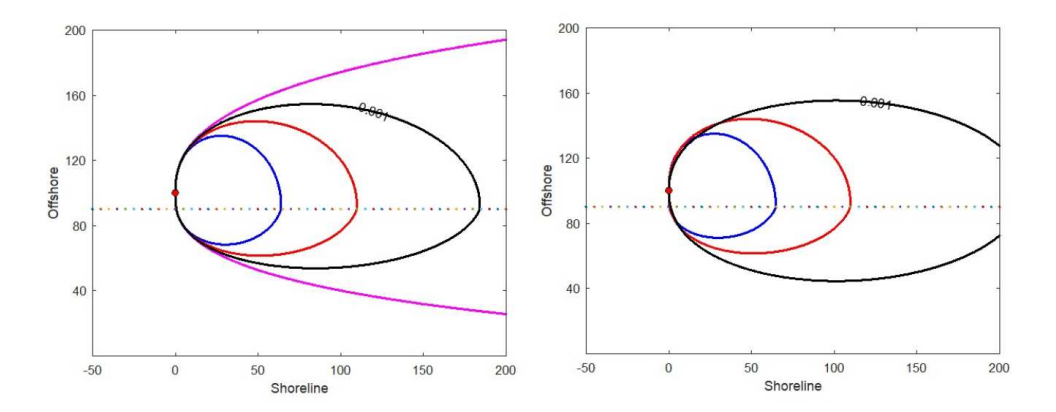


Figure 6: Contours of C=0.001 from a discharging point source at $\alpha=100$ on a step increase at $\ell=90$ when $\lambda=0.2$ and $\gamma=0.01$. (left column) The variation of decay with water depth when r=3 (top) and r=5 (bottom): $\sigma=-1/2$ (black), $\sigma=1/2$ (blue), $\sigma=3/2$ (red), and no effluent decay $\gamma=0$ (magenta). (right column) The variation of water depth when $\sigma=1/2$: r=1 (black), r=2 (red) and r=3 (blue).

To investigate the effect of effluent decay that increases with water depth, contours of concentration for discharging effluents from a point source at $\alpha=100$ on a step increase in water depth at $\ell=90$ are plotted in Figure 6 for $\sigma=-1/2$ (decay rate independent of depth), for $\sigma=1/2$ (decay rate linearly increases with depth) and for $\sigma=3/2$ (decay rate quadratically increases with depth).

The effect of variations in water depth on dispersing discharged effluent plumes is shown in Figure 6 (right) using the contour value of C = 0.001. If r > 3, we observed that only small portions of the plumes manage to enter and disperse in the shallow region.

By putting $Y = \ell$, we obtain the concentration at the discontinuity line

$$C_0(X,\ell) = C_1(X,\ell) = \frac{2}{r^2 + 1} \sqrt{\frac{\lambda}{4\pi X}} \exp\left\{-\gamma r^{\sigma} X - \frac{\lambda (\alpha - \ell)^2}{4r X}\right\},\,$$

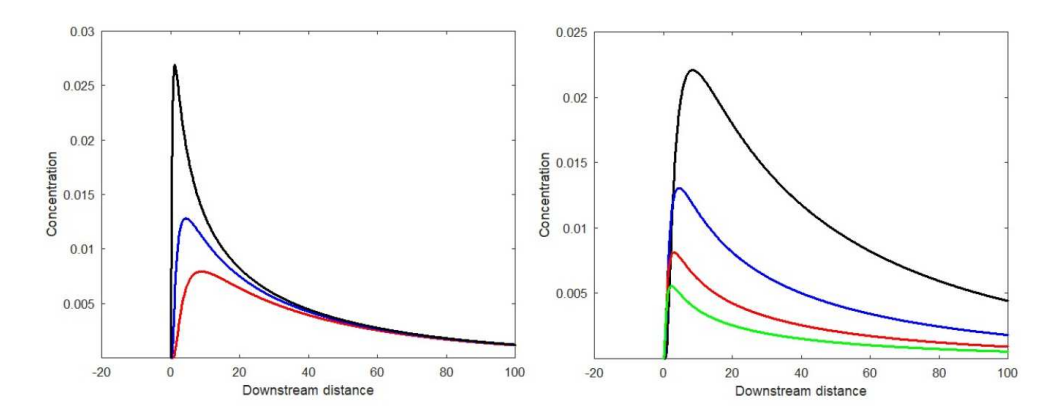


Figure 7: Concentration at the discontinuity line for discharging effluents with $\gamma=0.01$ and $\sigma=1/2$ on a step increase at $\ell=90$ when $\lambda=0.2$: (left) The location of a point source when r=2: $\alpha=95$ (black), $\alpha=100$ (blue) and $\alpha=105$ (red); and (right) The variation of water depth when $\sigma=1/2$ and $\alpha=100$: r=1 (black), r=2 (blue), r=3 (red) and r=4 (green).

which has a maximum value

$$C_{2\max} = \frac{2}{r^2 + 1} \sqrt{\frac{\lambda}{4\pi X_{2\max}}} \exp\left(-\frac{\sqrt{1 + 4\lambda \gamma r^{\sigma - 1} (\alpha - \ell)^2}}{2}\right)$$

at
$$X_{2 \max} = \lambda (\alpha - \ell)^2 / r \left[1 + \sqrt{1 + 4\lambda \gamma r^{\sigma - 1} (\alpha - \ell)^2} \right].$$

In the limit as $\ell \to 0$, we obtain the concentration at the shoreline

$$C_0\left(X,0\right) \approx \frac{2}{r^2+1} \sqrt{\frac{\lambda}{4\pi X}} \exp\left\{-\gamma r^{\sigma} X - \frac{\lambda \alpha^2}{4r X}\right\}.$$

For the case of no effluent decay ($\gamma = 0$), the maximum value

$$C_{2\max} \approx \frac{2\sqrt{r}}{r^2 + 1} \left(\frac{\alpha}{\alpha - \ell}\right) C_{*max} \text{ and } X_{2\max} \approx \frac{\lambda (\alpha - \ell)^2}{2r}.$$

If there is no depth change r=1 (and $\ell=0$), then $C_{2\max}\approx C_{*\max}$ and $X_{2\max}\approx X_{*\max}$.

The concentration at the discontinuity line for discharging effluents from a point source at $\alpha = 100$ with $\ell = 90$ and r = 3 is shown in Figure 7 (left).

The long tail of the graph is the result of the effluent plumes elongation in the downstream direction. The maximum concentration value is almost unaffected by increasing value of σ . The effect of increasing r for decay that linearly increases with depth ($\sigma=1/2$) is shown in Figure 7 (right). Due to small portions of discharged effluent plumes entering and dispersing in the shallow region, the maximum concentration that passes through the discontinuity line decreases from 0.0182 for r=1.5 to 0.0084 for r=3, a decrease of about 54%. We conclude that, in comparison to the discharged effluents from a point source at $\alpha=100$ on constant depth, the maximum concentration at the shoreline is greatly reduced as a result of a step increase in depth at $\ell=90$.

4. Concluding remarks

Mathematical models are presented using two-dimensional advection-diffusion equations to study the effects of a sudden water depth change and decay in mixing and dispersing steady discharged effluents through a sea outfall in coastal waters. Due to the small nature of decay rates, the effect of variability of loss of discharged effluents with depth from a short sea outfall are not enough to overcome the dispersion processes in the nearshore region due to no-slip condition at the shoreline. A large increase in water depth for more than three times that of the shallow region is needed to suppress the effect of no-slip condition.

For discharging effluents from a point source in the deeper region, the results show that in comparison to that of a flat seabed, the maximum concentration at the shoreline can be greatly reduced by the presence of a step increase in water depth. However, for discharging effluents in the shallow region, the effect is inversely proportional to the quadratic of depth ratio.

Acknowledgement

This work was supported by the Sultan Qaboos University Internal Grant IG/SCI/DOMS/18/04.

References

[1] P.J.W. Roberts, H.J. Salas, F.M. Reef, M. Libhaber, A. Labe, J.C. Thomson, *Marine Wastewater Outfalls and Treatment Systems*, International Water Association Publishing, London (2010).

- [2] Institution of Civil Engineers, Long Sea Outfalls, Thomas Telford Ltd., London (1989).
- [3] D.J. Gould, D. Munro, Relevance of microbial mortality to outfall design, Coastal Discharges - Engineering Aspect and Experience, Thomas Telford Ltd., London (1981), 45-50.
- [4] J.F. Macqueen, R.W. Preston, Cooling water discharges into a sea with a sloping bed, *Water Research*, **17**, No 4 (1983), 389-395; https://doi.org/10.1016/0043-1354.
- [5] D.A. Roberts, E.L. Johnston, N.A. Knott, Impacts of desalination plants discharges on the marine environment: A critical review of published studies, *Water Research*, 44 (2010), 5117-5128; https://doi.org/10.1016/j.watres.2010.04.036.
- [6] A. Purnama, H.H. Al-Barwani, Spreading of brine waste discharges into the Gulf of Oman, *Desalination*, 195, No 1-3 (2006), 26-31; https://doi.org/10.1016/j.desal.2005.09.036.
- [7] N. Ahmad, R.E. Baddour, A review of sources, diseffects. methods. and regulations of brine into marine posal envi-Ocean \mathcal{E} CoastalManagement, 87 (2014),1-7; https://doi.org/10.1016/j.ocecoaman.2013.10.020.
- [8] S. Lattemann, T. Hopner, Environmental impact and impact assessment of seawater desalination, *Desalination*, 220, No 1-3 (2008), 1-15; https://doi.org/10.1016/j.desal.2007.03.009.
- [9] P. Mebine, R. Smith, Effects of contaminant decay on the diffusion centre of a river, *Environmental Fluid Mechanics*, **6** (2006), 101-114.
- [10] P. Mebine, R. Smith, Effect of pollutant decay on steady-state concentration distributions in variable depth flow, *Environmental Fluid Mechanics*, 9 (2009), 573-586.
- [11] A. Kay, The effect of cross-stream depth variations upon contaminant dispersion in a vertically well-mixed current, *Estuarine and Coastal Shelf Science*, **24** (1987), 177-204.
- [12] R. Smith, Effects of non-uniform currents and depth variations upon steady discharges in shallow water, *Journal of Fluid Mechanics*, 110 (1981), 373-380.

- [13] A. Purnama, H.A. Al Maamari, E. Balakrishnan, Optimal outfall systems for nearshore effluent discharges on eroded sandy beaches, *Journal of Coupled Systems and Multiscale Dynamics*, 5, No 2-4 (2017), 217-224.
- [14] A. Purnama, H.A. Al-Maamari, E. Balakrishnan, Decay model for dispersion of coastal discharged effluents from multiport diffusers in the far-field, International Journal of New Innovations in Engineering and Technology, 12 (2019), 8-18.
- [15] A. Purnama, H.A. Al-Maamari, A.A. Al-Muqbali, E. Balakrishnan, The Effect of a step change in seabed depth on spreading discharged brine effluents from a two-outfall system, *Journal of Mathematical and Compu*tational Science, 10 (2020), 758-777; https://doi.org/10.28919/jmcs/4347.
- [16] D.A. Chin, P.J.W. Roberts, Model ofdispersion in coastal waters. Journal of Hydraulic Engineering, 111 (1985).12-28; https://doi/org/10.1061/(ASCE)0733-9429(1985)111:1(12).
- [17] I.R. Wood, Asymptotic solutions and behavior of outfall plumes, *Journal of Hydraulic Engineering*, **119** (1993), 553-580; https://doi.org/10.1061/(ASCE)0733-9429(1993)119:5(553).
- [18] C.H. Li, X.S. Pan, J. Ke, X.T. Dong, Comparison of 2D and 3D models of salinity numerical simulation, *Polish Maritime Research*, **22**, No S1 (2015), 26-29; https://doi.org/10.1515/pomr-2015-0028.
- [19] D.L. Craig, H.J. Fallowfield, N.J. Cromar, Comparison of decay rates of faecal indicator organisms in recreational coastal water and sediment, Water Supply, 2 (2002), 131-138; https://doi.org/10.2166/ws.2002.0095.
- [20] A. Adcroft, R. Hallberg, J.P. Dunne, B.L. Samuels, J.A. Galt, Simulations of underwater plumes of dissolved oil in the Gulf of Mexico, Geophysical Research Letters, 37 (2010), L18605; https://doi.org/10.1029/2010GL044689.
- [21] V.P. Shukla, Analytical solutions for unsteady transport dispersion of non-conservative pollutant with time-dependent periodic waste discharge concentration, *Journal of Hydraulic Engineering*, **128** (2002), 866-869.
- [22] D.W. Ostendorf, Longshore dispersion over a flat beach, *Journal of Geo*physical Research, 87 (1982), 4241-4248.